ARTICLE

Pressure Impulse during Explosive Boiling on the Surface of a High Temperature Melt in Water—Discussion of the Calculation Model

Yuri Ivochkin[1], Igor Teplyakov[1], Oleg Sinkevich[1,2], Sergei Shchigel[1] and Stepan Yudin[1,2,*]

[1]Heat Transfer in Power Plants Laboratory, Joint Institute for High Temperatures, Moscow, 125412, Russia

[2]Department of Engineering Thermophysics, National Research University "Moscow Power Engineering Institute", Moscow, 111250, Russia

*Corresponding Author: Stepan Yudin. Email: yudin_uchebnaya@mail.ru

ABSTRACT

This study explores the mechanism behind the generation of pressure pulses on the outer surface of a molten metal droplet when immersed in water. The absence of any external trigger is assumed, and the droplet is surrounded by a vapor layer with surface hydrodynamic waves at the vapor-liquid interface. The study examines the heating conditions of a cylindrical column of water used to model a volume of cold liquid interacting with a hot metal surface, which explosively boils upon direct contact. Within the framework of classical homogeneous nucleation theory, the relationship between pressure pulse magnitude and rise time and the size of the contact area and surface temperature of the droplet is established. A criterion for determining the magnitude of the pressure pulse is derived, showing that significant pressure pulses occur within a narrow range of values for this criterion. Experimental investigations have been conducted to measure the key parameters—such as the duration and area of contact and pressure amplitude buildup—when room-temperature water comes into contact with a hot steel surface. The experimental results are compared with the theoretical predictions. Incorporating Skripov's theory of explosive boiling into the model helps explain the relationship between the pressure pulse and contact area, only when the droplet surface temperature is near or exceeds the temperature of the maximum possible water superheating.

KEYWORDS

Vapor explosion; fragmentation; contact diameter; delay time; superheated water

Nomenclature

C	Speed of sound
C_p	Heat capacity at constant pressure
D	Diameter of contact spot
L	Heat of vaporization
P	Pressure
R	The radius of vapor bubble
R_g	Gas constant
T	Temperature

T_*	Temperature in the liquid at the time of boiling
T_s	Temperature of saturation
ΔT	Depth of entry into the metastable region
a	Thermal diffusivity
h	Height of a cylindrical volume of liquid
k	Thermal conductivity
q	Heat flux density
r	Radial distance in a cylindrical coordinate system
t	Time
t''	The boiling time of the entire liquid
z	Axial coordinate in a cylindrical coordinate system

Greek Symbols

α_v	Overheated vapor thermal diffusivity as a function of temperature
θ	Time from the beginning of the contact
ρ	Density
υ	Specific volume
$\overline{\Omega}$	The number of ready-made centers per unit volume

Subscripts and Superscripts

0	Cooling water
m	Melted liquid droplet
gr	Contact area
l	Direction from water side
υ	Direction from vapor side
n	Normal direction to the surface
s	Spherical coordinate system
′	Water
″	Vapor
cent	Center of hemispherical steel heated body
surf	Surface of hemispherical steel heated body
bubble	Bubble
max	Maximum value
means	Measured value
del	Delay
cont	Contact
interphase	Interphase

1 Introduction

The relevance of the study of the emergence and development of a pressure pulse on the high-temperature surface of a molten metal drop immersed in water (without an external trigger) is related to the problem of the occurrence of a vapor explosion in emergencies in various industries, including nuclear power and metallurgy. A detailed description of this problem, applied mainly to the safety issues of nuclear power plants, can be found in early review papers [1–3]. Modern information on this problem is presented in reviews [4–6]. The results of studies of steam explosions, as applied to

metallurgy, are described in [7]. A review of works on the study of heat transfer peculiarities at steam explosions is presented in [8].

In the literature, there is a large amount of experimental data on the interaction of a drop of molten metal with a cooling liquid—usually water at room temperature. In experiments, mainly liquid tin drops falling into the sea [9] or ordinary [10–14] water as well as materials based on lead [13] and bismuth [15–17] have been used. Droplets made of copper [18,19] and iron melts [7,20] have been used to model processes at high temperatures. A comparative analysis of the fragmentation process of iron and corium droplets carried out taking into account heat transfer by radiation, is presented in [21].

In addition to nuclear power and metallurgy, steam explosions have been observed in the paper industry, as well as in the production and transportation of liquefied natural gas [22]. The results of a series of studies on modeling steam explosions in manufacturing paper are presented in [23–26]. In these experiments, performed with drops of table salt falling into the water, it is confirmed that spontaneous steam explosions can be initiated by the accidental crushing of a single drop. A distinctive feature of steam explosions in the interaction of liquefied natural gases with water is the absence (due to the low cryogenic temperatures of the coolant) of the influence of thermal radiation on the process of their occurrence. Possible vapor explosions in devices using liquid sodium as a coolant, such as fast reactors, are discussed in [27].

In most of the experiments performed, in addition to visual observations, temperature characteristics of the process and pressure pulses were measured. In some experiments [14,28,29], along with conventional video cameras, cameras operating in the range of X-rays were used, which made it possible to significantly improve image analysis by separating vapor from metal fragments. More than a dozen physical models devoted to droplet fragmentation can be found in the literature. Among them, one can single out the models based on: the penetration of coolant jets into the volume of the droplet [30], and its destruction due to both internal boiling (cavitation) [31] and thermomechanical stresses during abrupt cooling [32]. The above models describe the initial stage of the fragmentation process with different approximations and are mainly descriptive (and to some extent contradictory) in nature.

Droplets of melted material being immersed in water are surrounded by a vapor film, the boundary of which oscillates with great or small amplitude. Then, if there is a trigger (for example an external pressure impulse), the vapor film surrounding the droplet is destabilized. Thus, the oscillations of the phase boundary may reach a large scale and liquid may approach or touch the heated droplet surface. So, the explosive boiling of the liquid fraction contacting with the metal surface becomes possible. It leads to pressure impulse generation, which causes the fragmentation of the droplet. In addition, an initial pressure impulse generates an acoustic wave in the liquid and the melted droplet. This wave may affect the vapor films around neighboring particles of melted material. It may intensify the process of steam explosion. A detailed description of this behavior of the steam layer, as well as its explosive destruction, is described in [33].

The vapor film oscillations (without external trigger) may appear as a result of a hydrodynamic effect if the droplets are passed over by the liquid flow (instabilities of Kelvin-Helmholtz), or as a result of thermal processes that take place at the liquid-vapor phase boundary (in this case there is a wider circle of phenomena than Rayleigh-Taylor instability).

The object of this work is an investigation of the pressure impulse generation value, the conditions of its generation and the duration of explosive water boiling at the high temperature melted droplet surface (according to [34]). We think that, under some circumstances, this pressure impulse may be the trigger of steam explosion and may cause droplet fine fragmentation.

2 Model Description

When water contacts the melted droplet surface due to surrounding vapor film destabilization (the simplest model of the phenomenon is shown in Fig. 1), the pressure impulse may appear. It is connected with explosive boiling, and a rapid decrease in volume density is considered. The formed vapor bubble (expanding at the speed of sound) in some cases does not compensate for the increasing pressure.
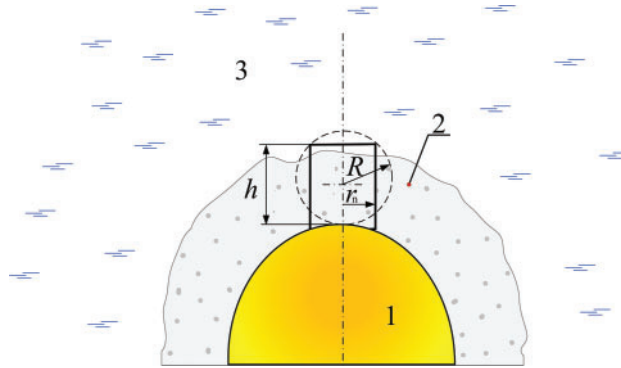
Figure 1: Simplified scheme of water explosive boiling after vapor film continuity breakdown; 1—melted droplet, 2—vapor film, 3—cooling water

There is now a fairly large number of experimental studies of the effects of the vapor film surrounding a drop of heated metal when it enters a coolant. These experimental data, and several qualitative considerations by various authors, show that many mechanisms lead to the effect of the vapor film on the deformation (fracture) of the liquid metal droplet when it interacts with the surrounding liquid.

In the first part of this paper, an attempt is made to evaluate the effect of the vapor film during the transition of a liquid to a metastable state within the framework of the well-known V.P. Skripov model [34].

2.1 The Peculiarities of Heat Transfer Regime

Instabilities of vapor film surrounding the droplet, which may lead to direct contact between water and the hot surface of molten metal (as mentioned above), are described in works [8,35].

Consider heating a water cylinder and its contact with a hot droplet surface. The cylinder models the water volume (which has, in general, a more complicated form). Several mechanisms produce explosive boiling. One of them is related to pressure entry into the metastable zone, which is known to lead to boiling. A necessary condition for explosive boiling, according to [34], is a sufficiently deep entry into the metastable zone, since:

$$T^* - T_s = \frac{\beta L}{\overline{C_p}}, \tag{1}$$

where L, T^*, T_s and $\overline{C_p}$ are the specific heat of evaporation, temperature of superheated water, saturation temperature, mean heat capacity; $\beta = 0.42$ for water at atmospheric pressure. It means, in our case, that superheating must be about 200 K.

It was noted in [34] that the liquid can be superheated even in the presence of artificial centers if heating occurs quickly enough. Moreover, it is necessary to provide such a heating rate, which noticeably exceeds the heat consumption for evaporation on active centers. The analytical solution for two semi-infinite bodies was used to estimate the heating rate of the cylinder and to determine the temperature at the phase boundary. It was also used to determine the boundary condition on the lower surface of the cylinder, the temperature of which is assumed not to exceed the temperature of the limiting overheating of the coolant, as well as to verify the numerical solution for the case of zero heat flow on the side surface of the cylinder. The solution to this problem for the initial temperature distribution independent of the coordinate is found by [36]:

$$\frac{T - T_0}{T_{gr} - T_0} = \mathrm{erf}\ (Z), Z = \frac{z}{2\sqrt{a\theta}}. \tag{2}$$

The heat flux on the droplet surface is:

$$q_1 (0,\ \theta) = \frac{k\left(T_{gr} - T_0\right)}{\sqrt{\pi a\theta}}. \tag{3}$$

Conjugating by heat flux, temperature in the contact zone is:

$$T_{gr} = T_0 + \frac{(T_m - T_0)}{1 + \left(\dfrac{(k\rho C_p)_0}{(k\rho C_p)_m}\right)^{\frac{1}{2}}}, \tag{4}$$

where θ, k, a, T_{gr}, T_m, T_0, ρ, and C_p are the time from the moment of contact, thermal conductivity, thermal diffusivity, temperature at the interphase zone contact, molten droplet temperature, cooling water temperature, density, thermal capacity; index «0» refers to cooling liquid, index «m» refers to melted droplet, z—the coordinate normal to the droplet surface; $T = T (z, \theta)$ temperature as a function of time and coordinate normal to the droplet surface.

Figs. 2 and 3 (which illustrates calculations by Eqs. (3)–(5)) show heat flux density variation at the phase boundary and time dependency of temperature in the water cylinder at the z–coordinate 3 μm from the surface. The heat flux decreases several times (Fig. 2) during 1 ms (due to low water thermal conductivity) while the temperature of the metal surface and contact zone change slightly. However, the water cylinder becomes superheated for approximately 200 K at the mentioned coordinate.

For a more exact definition of the temperature distribution of a water cylinder in contact with a droplet surface, the heat conduction equation was solved in cylindrical coordinates:

$$\frac{\partial T}{\partial t} = a_v \left(\frac{1}{r}\frac{\partial}{\partial r}\left(r\frac{\partial T}{\partial r}\right) + \frac{\partial^2 T}{\partial z^2}\right),$$

with the following boundary conditions:

$z = 0$: $T = T_{gr}$;

$z = h$: $T = T_0$;

$r = r_n$: $q_l = q_v$,

where z, r, h, r_n, T_0, a_v, q_l and q_v are the coordinate normal to the droplet surface ($z = 0$ in the point of inter-phase contact), coordinate along the radius of cylinder ($r = 0$ at the symmetry axis), height of the cylinder, which is approximately equal to the vapor film thickness, cylinder radius, cooling water

temperature, thermal diffusivity (here we considered as constant), heat flux densities at the lateral cylinder surface in liquid and vapor correspondingly.
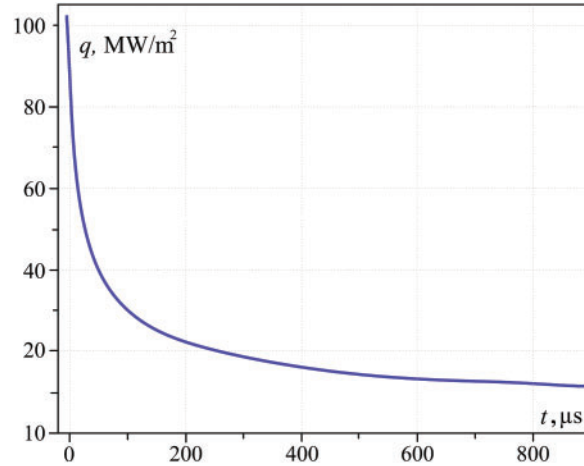
Figure 2: Heat flux dependence on time in contact zone ($z = 3\ \mu m$; $T_{gr} = 584$ K)
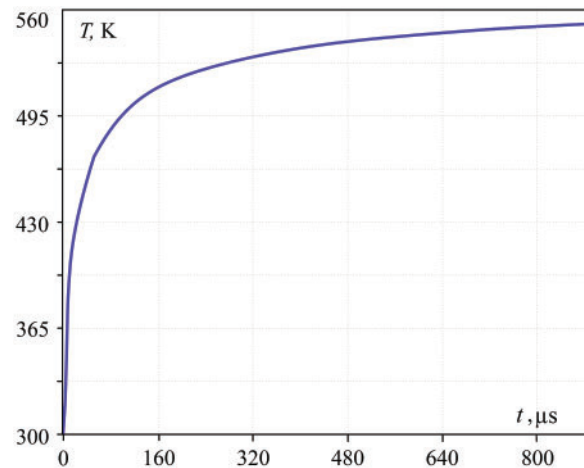
Figure 3: Droplet surface temperature dependence of time ($z = 3\ \mu m$; $T_{gr} = 584$ K)

To determine the boundary conditions on the side surface of the cylinder, the temperature distribution in the vapor film was found. The problem was solved in a one-dimensional approximation in polar coordinates taking into account the temperature variability of superheated vapor properties:

$$\frac{1}{r_s}\frac{\partial}{\partial r_s}\left(a_v\left(T\right)r_s\frac{\partial T}{\partial r_s}\right) = 0$$

where r_s, $a_v\left(T\right)$, T are the distance from droplet center, overheated vapor thermal diffusivity as a function of temperature, temperature as a function of r_s in the vapor film.

For numerical calculation, the appropriate explicit schemes of second order for cylinder and polar coordinates were used [37].

Hereinafter, we determine the experimental heating period between the water contact with the droplet surface and the start of explosive boiling, which is measured by the fall of electrical resistance between the droplet and liquid. Correspondingly, the height of the water cylinder in a metastable state is determined, and the overheating satisfies the explosive regime conditions [34].

It is possible to calculate the radius of the sphere (R), the volume of which is equal to the volume of the water cylinder part in which explosive boiling is realized.

The parameter R is used in subsequent dimensionless analysis.

For example, for the following calculation, the temperature of the tin droplet was chosen so that the temperature of the interphase surface corresponds to the ultimate overheating water temperature 311K. Experimental waiting time is assumed to be 1 ms.

The results of calculations for the above example are represented in Fig. 4. The line (2) in Fig. 4 cuts part of the water cylinder heated to the metastable condition that satisfies the condition of explosive boiling [34].
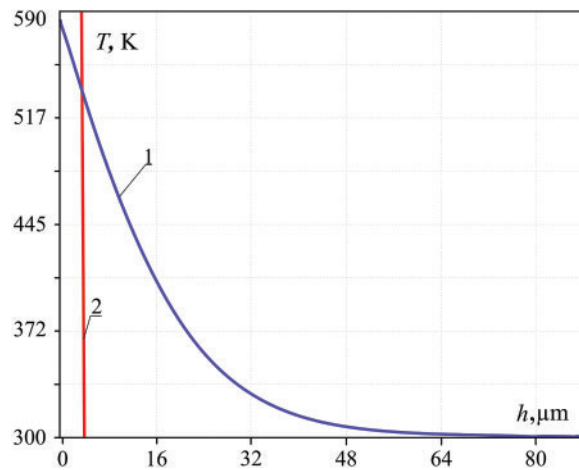
Figure 4: Temperature distribution (1) along the height of the water cylinder (h) at symmetry axis after 1 ms from water droplet surface contact; to the left of (2)—the zone of explosive boiling; ($T_{gr} = 584$ K, $t = 1$ ms)

2.2 Pressure Impulse

The time of superheated liquid explosive boiling out at the active centers, according to [30], is:

$$t'' = \frac{1}{\varphi^{\frac{1}{n}}} \left(\frac{\rho'}{\rho''} \frac{3}{4\pi \overline{\Omega}} \right)^{\frac{1}{3n}},$$ (5)

where $\overline{\Omega}$, ρ' and ρ'' are the number of active centers per volume unit, densities of liquid and vapor correspondingly.

The number of active centers to the moment of explosive boiling beginning is determined as an integral of nucleation speed according to classic theory of homogenous nucleation. Then (the Raleigh case): $n = 1$. In [30], the law of bubble growth is represented as: an asymptotical Raleigh law for bubble growth.

$$R_{bubble} = \varphi t^n; R_{bubble} = \sqrt{\frac{2\Delta P}{3\rho'}} t.$$

For a first estimation, φ may be determined from the following considerations [38]:

$$\frac{\partial P}{\partial T} = \frac{L}{T\left(v'' - v'\right)} - \text{ Klaiperon } - \text{ Clausius equation.}$$

If we assume in the zone of heating $\frac{\partial P}{\partial T} \approx const \approx \frac{\Delta P}{\Delta T}$, then:

$$\Delta P = \frac{\Delta T L}{T\left(\frac{1}{\rho''} - \frac{1}{\rho'}\right)}, \tag{6}$$

where L is the heat of vaporization.

The formed vapor spherical bubble expands at the speed of sound, so we'll describe the growth of its radius R as:

$$\Delta R = C t'', \tag{7}$$

here ΔR is the radius enlarging to the moment of the end of boiling or, putting new variables:

$$B = \left(\frac{3}{4\pi\overline{\overline{\Omega}}}\right)^{\frac{1}{3}}; x = \left(\frac{\rho'}{\rho''}\right)^{\frac{1}{3}},$$

We have:

$$\Delta R = \frac{CBx}{\varphi} = \frac{CBx}{\sqrt{\frac{2\Delta T L}{3T\left(x^3 - 1\right)}}}. \tag{8}$$

Defining K, as:

$$K = \frac{C}{R}\left(\frac{3}{4\pi\overline{\overline{\Omega}}}\right)^{\frac{1}{3}}\sqrt{\frac{3T}{2\Delta T L}}, \tag{9}$$

We have the following equation:

$$\left(1 + Kx\sqrt{\left(x^3 - 1\right)}\right)^3 = x^3. \tag{10}$$

Since only positive x are of interest, it may be written:

$$1 + Kx\sqrt{\left(x^3 - 1\right)} = x.$$

Then:

$$\sqrt{\frac{x^3 - 1}{\left(x - 1\right)^2}} = \frac{1}{K} = \sqrt{\frac{x^2\left(x^2 + x + 1\right)}{x - 1}} = \frac{R}{C}\left(\frac{4\pi\overline{\overline{\Omega}}}{3}\right)^{\frac{1}{3}}\sqrt{\frac{2\Delta T L}{3T}}$$

or

$$R = \sqrt{\frac{x^2 (x^2 + x + 1)}{x - 1}} C \left(\frac{3}{4\pi \overline{\Omega}} \right)^{\frac{1}{3}} \sqrt{\frac{3T}{2\Delta TL}}, \tag{11}$$

where T, ΔT, L, C, R_g and K are the vapor temperature, the level of superheating, specific heat of vaporization, speed of sound, vapor gas constant and the dimensionless criterion K (9), which depends upon contact spot radius and droplet surface temperature.

Then the Eq. (10) is solved for x, and thus the vapor density is determined in the enlarged bubble to the end of boiling (ρ'') as a function of K. So, one can determine the pressure in the bubble (12), and it is the pressure impulse, which determines the following events:

$$P'' = \rho'' R_g T. \tag{12}$$

The duration of the impulse (the duration of pressure growth inside the bubble until it reaches maximum value) is:

$$t'' = \frac{1}{\sqrt{\frac{2}{3\rho_l} \frac{\Delta T}{T \left(\frac{1}{\rho''} - \frac{1}{\rho'} \right)}}} \left(\frac{\rho'}{\rho''} \frac{3}{4\pi \overline{\Omega}} \right)^{\frac{1}{3}}, \tag{13}$$

Bellow the dependence of pressure impulse (Fig. 5) and duration of pressure growth in the bubble (time of boiling out) (Fig. 6) are given as a function of sphere radius (R), the volume of which equals the initial volume of the explosive boiling liquid. This dependence refers to the temperature of the contact zone to be the maximum water overheating level at atmospheric pressure and experimental time of water cylinder heating.
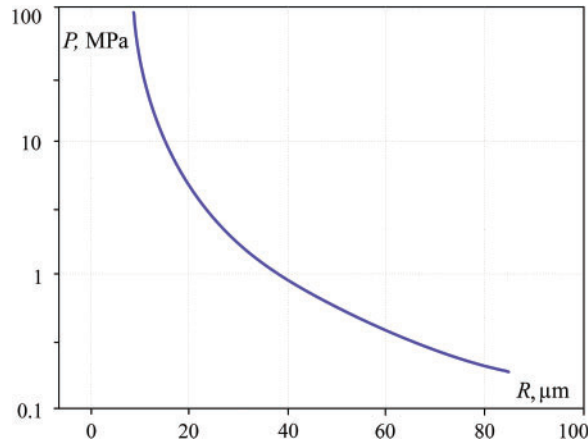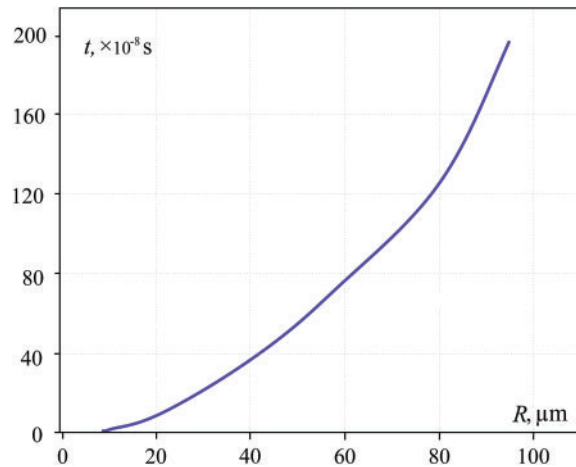

**Figure 5:** Pressure impulse dependency upon R

The dependence between vapor density and criterion K (Fig. 7) is physically restricted by the maximum possible vapor density at critical water temperature.

It should be noted that there are some problems with the model based on the mechanism described in [34]. One of them is related to the need to know the number of nucleation centers, which for various experiments is known with insufficient accuracy. Another problem is the need for the liquid to enter the metastable zone. In addition, the Skripov model does not take into account the influence of vapor

film oscillations (small and with finite amplitude) on the development of instabilities not related to the metastable state of the liquid. Thus, the results presented here demonstrate the main difficulties of the droplet fragmentation model based on shock boiling theory [34]. However, there are other models available. Most notably, in reality, each type of boiling nucleation is heterogeneous. Therefore, the model must include either a heterogeneous factor (the value of which is usually unknown in advance) or there must exist an alternative model of heterogeneous nucleation.

Figure 6: Time of pressure growth (the time of boiling out) in pressure impulse as a function of R
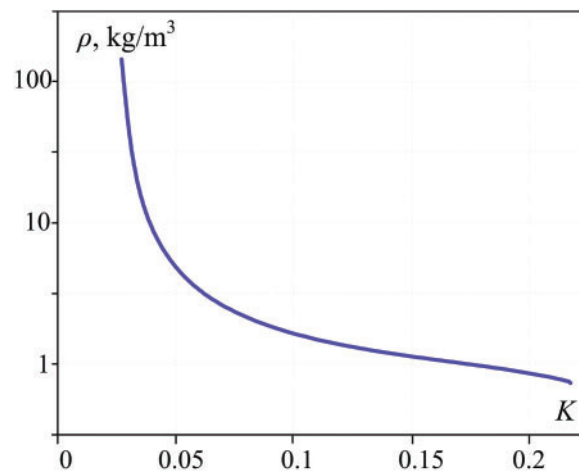

Figure 7: Vapor density (at the end of boiling) dependency upon dimensionless parameter K

Estimated calculations within the framework of the simplest V.P. Skripov model show its limitations. The essence of its limitations is that it is based on homogeneous nucleation liquid; therefore, a more detailed analysis of other mechanisms is required, some of which have been partially discussed, some of which have not. The analysis of such mechanisms is the aim of further research.

3 Experimental Data

Based on the results of experiments with metal balls [39–41], it can be assumed that the processes of destruction of vapor shells of the coolant near the superheated surfaces of solid and liquid metallic bodies develop similarly. Therefore, additional experiments modeling the initial stage of vapor film destruction on a hot liquid-metal drop and intended to verify the results of the above deductions were performed under conditions of explosive boiling of water on solid samples of hemispherical shape. Experiments using a similar measurement technique were performed earlier in [42].

The scheme of the experimental setup and the main measurements carried out on it are shown in Fig. 8. The working section was a cylindrical rod, the lower end part of which was made of stainless steel AISI 304. The end surface of the cylinder had the shape of a hemisphere with a diameter of 10 mm. The working section, thermally insulated over the entire surface, except for the hemispherical part, was heated by direct electric current, which was passed through an electrically insulated spiral wound on its surface.
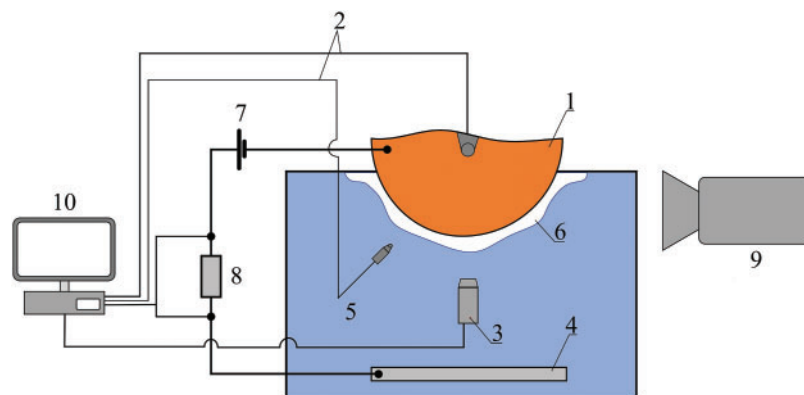
Figure 8: Scheme of the experimental setup and main measurements. 1—sample; 2—thermocouple (K-type); 3—pressure sensor; 4—electrode; 5—water; 6—steam shell; 7—battery: 8—reference resistor; 9—video camera; 10—computer

The experiments were performed in the following sequence. In the initial (raised) position, the working section was heated in air to a temperature of ~773K. After that, the electric heater was switched off, and the hot working section was immersed in the bath filled with distilled water to the depth of the hemisphere radius with the help of a special coordinate device at a speed of several millimeters per second. This method of heating was a simple way to affect the mode of stable film boiling near the hot hemisphere, and also to allow explosive escape of the vapor film from the heated surface of the working section during the cooling process. Distilled water at room temperature (291K) (degassed using two-hour boiling) was used in the experiments.
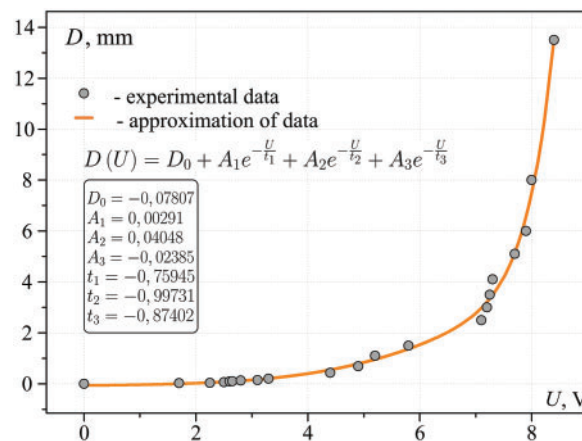
Temperature measurements were made with the help of chrome-alumni thermocouples, the junction of which were placed in water, in the center of the hemisphere, and different parts of the working area. This made it possible to control with sufficient accuracy the value of heat flux density on the hemispherical surface in the film boiling mode. The estimated value of the temperature of the hot surface of the sample was determined computationally by solving the unsteady heat conduction equation.

In the experiments, pressure pulses were investigated, which were generated at the collapse of the vapor cavity in the process of cooling the working section. High-frequency piezoelectric transducers

from PCB PIEZOTRONICS Model: HS113A28, which were located at a distance of 6 mm from the lower end of the hemisphere, were used as pressure transducers.

In addition to pressure transducers, the conductometric technique of determining the parameters of water contact with the heated surface was used in the experiments. The characteristics of this process (area and duration of contact) were determined by the change in the value of the voltage drop on the "exemplary" resistance, which is part of a closed electrical circuit consisting of a direct current source, two electrodes (one of which is the working area and the other is a copper plate placed in water), connecting wires, volumes of water and water vapor. In the absence of water contact with the heater, the total resistance of the circuit, determined by the electrical resistance of the vapor layer, is as large as possible, and the current and voltage drop across the reference resistance are minimal.

At the moment of contact of the heater with water in the measuring circuit the electric current increases sharply, the value of which varies depending on the contact area. The calibration dependence of the voltage drop across the sample resistance on the equivalent diameter of the contact area (Fig. 9) was obtained in a specially designed experiment in which the contact spot was modeled by the area of the end surface of a copper wire insulated from the sides. One of the ends of a piece of wire, which diameter in the experiments varied from 30 μm to 15 mm, was fixed on the hemispherical surface of the working area, and the other was immersed a few millimeters into water.

$$D(U) = D_0 + A_1 e^{-\frac{U}{t_1}} + A_2 e^{-\frac{U}{t_2}} + A_3 e^{-\frac{U}{t_3}}$$

$D_0 = -0,07807$
$A_1 = 0,00291$
$A_2 = 0,04048$
$A_3 = -0,02385$
$t_1 = -0,75945$
$t_2 = -0,99731$
$t_3 = -0,87402$

Figure 9: Calibration dependence of the contact diameter on the voltage drop across the reference resistor

Based on the results of video observations (video recording frequency 1000 fps), it was found that the contact of the cooler with the hot surface takes place in the lowermost part of the hemispherical sample, where the thickness of the vapor shell is minimal. The experiments used National Instruments equipment, and the measurements were performed using the Labview software environment. The frequency of digitization of signals from pressure and contact sensors was 5×10^5 Hz.

A characteristic form of oscillograms of pressure P_{meas} and the equivalent diameter of the contact spot D_{cont}, measured at three different temperatures in the center of the heated sample T_{cent}, are presented in Figs. 10–12. As can be seen from the presented graphs, for all three values of T_{cent}. There is a time delay t_{del}. Pressure curve relative to the oscillogram of the contact diameter. Table 1 presents the characteristic values t_{del} and the contact radius obtained taking into account the calibration dependence in Fig. 9. The same table presents the estimated temperatures of heated metal T_{surf} and interphase $T_{interphase}$, (at the moment of contact of water with a hot body) surfaces, as well as the pressure

at the explosion point P, calculated taking into account the pressure drops according to the law $P_{meas} \sim P/r$. Here r is the distance from the explosion point to the measurement point (in our case, $r = 5$ mm).
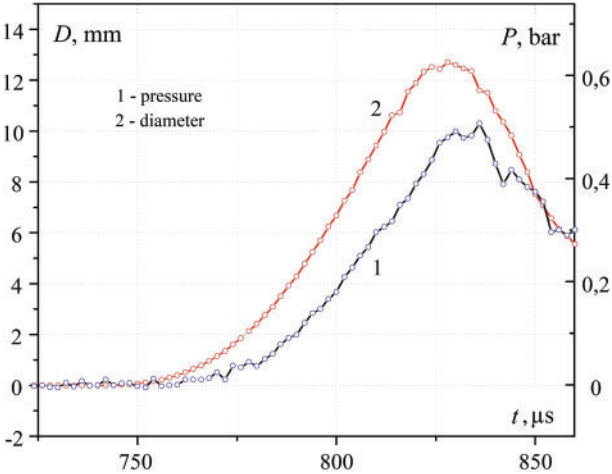
Figure 10: Change over time of pressure (1) and diameter of contact (2) during the initial interaction of water (temperature $T \sim 293$ K) with hot steel surface (549 K)
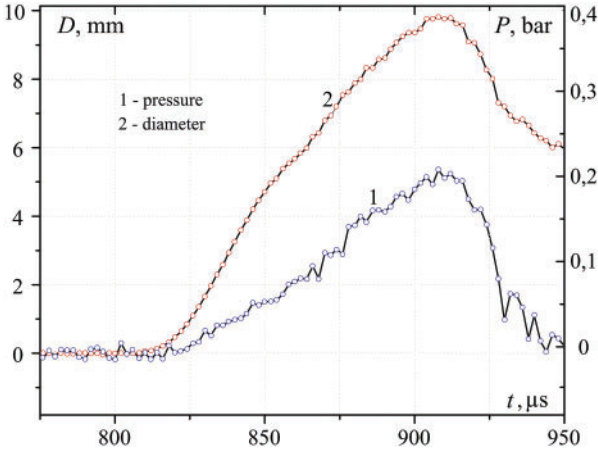
Figure 11: Change over time of pressure (1) and diameter of contact (2) during the initial interaction of water (temperature $T \sim 293$ K) with hot steel (599 K) hemisphere
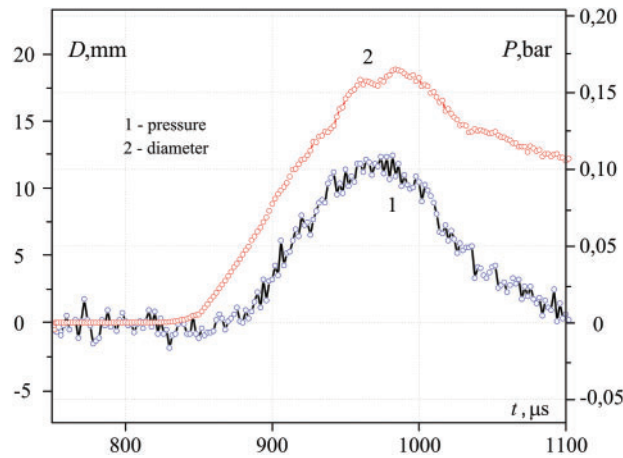
Figure 12: Change over time of pressure (1) and diameter of contact (2) during the initial interaction of water (temperature T∼293 K) with hot (489 K) steel hemisphere

Table 1: Characteristic values of the main interaction parameters

T_{cent}, K	T_{surf}, K	$P_{max.meas}$, bar	P, bar	t_{del}, μs	$(D/2)_{cont}$, μm	$T_{interphase}$, K
489	472	0,1	1,6	20	500	469
549	530	0,5	8,0	12	250	521
599	564	0,2	3,2	8	100	561

The experimental results obtained confirm that the delay time of explosive boiling increases with increasing contact patch, which, in turn, decreases with increasing temperature of the hot surface. The dependence $P(T_{cent})$ has a maximum, that is, the pressure amplitude can change in different directions depending on the temperature of the hot surface.

As mentioned above, the comparison of experimental and analytical dependences is relatively restricted nevertheless, it may be marked that there is a good correspondence between pressure impulse value at various squares of contact at the surface temperature close to the temperature of the maximum possible temperature of water overheating. At the same time, the analytical period of pressure growth in pressure impulse is several times less than the experimental one.

The analysis of the experimental data on the pressure rise generated by the boiling liquid at its contact with the heated metal surface given in the current section shows that the model based on the transition of the liquid to a metastable state (explosive boiling) does not allow to describe the observed experimental results accurately enough, in particular, the sharp pressure rise in the boiling region is not clear enough.

4 Conclusions

The paper proposes and describes a model of pressure pulse formation on the surface of a high-temperature melt drop when it is immersed in water. The model is based on the explosive boiling of coolant at the wave crests generated at the vapor-liquid interface, where it comes into contact with a hot metal surface. Within the framework of the explosive boiling theory based on the classical

concept of homogeneous nucleation, a criterion determining the magnitude of the pressure pulse and depending, in particular, on the size of the contact spot and the number of vaporization centers is determined. It is shown that significant pressure pulses occur in a rather narrow range of values of this criterion. Additional experiments have been carried out to determine the main parameters (duration and area of contact, pressure amplitude increase) of the contact of room temperature water with a hot steel surface. The theoretical relationship between the intensity of the pressure pulse and the volume of the boiling liquid, as well as the temperature of the droplet surface, has been established. These calculations enable the determination of the contact spot area corresponding to the observed pressure (P) in the experiment. It should also be noted that the proposed model has several disadvantages associated, in particular, with the absence in the literature of detailed information on the boiling centers, which are little known for specific experiments. In addition, the proposed model does not take into account the influence of both small and finite amplitude vapor film oscillations on the development of instability. The results obtained indicate the need for a deeper study of the nature of the vapor film instability since the area of the hot metal contact with the liquid formed as a result of wave motion largely determines the intensity of the resulting pressure pulse.

Author Contributions: The authors confirm contribution to the paper as follows: study conception, mathematical model and analysis: Oleg Sinkevich, Sergei Shchigel, Yuri Ivochkin; data collection: Yuri Ivochkin, Igor Teplyakov; analysis and interpretation of results: Yuri Ivochkin, Stepan Yudin, Igor Teplyakov; computational model and calculations: Stepan Yudin; draft manuscript preparation: Yuri Ivochkin, Stepan Yudin. All authors reviewed the results and approved the final version of the manuscript.

Availability of Data and Materials: No data was used for the research described in the article.

Ethics Approval: Not applicable.

References

1. Fletcher DF, Theofanous TG. Heat transfer and fluid dynamic aspects of explosive melt–water interactions. Adv Heat Transf. 1997;29:129–213. doi:10.1016/S0065-2717(08)70185-0.
2. El-Genk MS, Matthews RB, Bankoff SG. Molten fuel-coolant interaction phenomena with application to fuel safety. Prog Nucl Energy. 1987;1(2–4):151–98. doi:10.1016/0149-1970(87)90005-9.
3. Berthoud G. Vapor explosions. Annu Rev Fluid Mech. 2000;32:573–611. doi:10.1146/annurev.fluid.32.1.573.
4. Melikhov VI, Melikhov OI, Yakush SE. Thermal interaction of high-temperature melts with liquids. High Temp. 2023;60(2):252–85. doi:10.1134/S0018151X22020274.
5. Simons A, Bellemans I, Crivits T, Verbeken K. Vapor explosions: modeling and experimental analysis in both small- and large-scale setups: a review. JOM. 2021;73(10):3046–63. doi:10.1007/s11837-021-04767-y.

6. Melikhov VI, Melikhov OI, Yakush SE. Hydrodynamics and thermophysics of steam explosions. Report "IPMech RAN". Moscow; 2020. p. 1–276 (In Russian).

7. Li M, Chen Z, Liu L, Shen Z, Wang C. Fragmentation and solidification of fuel-coolant interaction of columnar molten iron and water. J Therm Anal Calorim. 2023;148:10897–906. doi:10.1007/s10973-023-12419-3.

8. Simons A, Bellemans I, Crivits T, Verbeken K. Heat transfer considerations on the spontaneous triggering of vapor explosions—a review. Metals. 2021;11:55. doi:10.3390/met11010055.

9. Deng Y, Guo Q, Xiang Y, Fang D, Ma W. Experimental study on steam explosion of multiple droplets in different chemical solutions. Int J Heat Mass Transf. 2024;226:125477. doi:10.1016/j.ijheatmasstransfer.2024.125477.

10. Simons A.Bellemans I, Crivits T, Verbeken K. The effect of vapour formation and metal droplet temperature and mass on vapour explosion behavior. Int J Heat Mass Transf. 2022;196:12328. doi:10.1016/j.ijheatmasstransfer.2022.123289.

11. Wang C, Wang C, Chen B, Li M, Shen Z. Fragmentation regimes during the thermal inter-action between molten tin droplet and cooling water. Int J Heat Mass Transf. 2021;166:120782. doi:10.1016/j.ijheatmasstransfer.2020.120782.

12. Dullforce TE, Buchanan DJ, Perckover RS. Self-triggering of small-scale fuel-coolant interactions: I. Experiments. J Phys D Appl Phys. 1976;9(9):1295–303. doi:10.1088/0022-3727/9/9/006.

13. Wang C, Wang C, Chen B, Lin D, Li M, Shen Z. Comparative study of water drop let interactions with molten lead and tin. Eur J Mech/B Fluids. 2020;80:157–66. doi:10.1016/j.euromechflu.2019.11.010.

14. Pak HS, Hanson RC, Sehgal DR. Fine fragmentation of molten droplet in subcooled water due to vapor explosion observed by X-ray radiography. Exp Therm Fluid Sci. 2005;29(3):351–61. doi:10.1016/j.expthermflusci.2004.05.013.

15. Kouraytem N, Li EQ, Thoroddsen ST. Formation of microbeads during vapor explosions of Field's metal in water. Phys Rev. 2016;93:063108. doi:10.1103/PhysRevE.93.063108.

16. Tan S, Zhong Y, Cheng H, Cheng S. Experimental investigation on the characteristics of molten lead-bismuth non-eutectic alloy fragmentation in water. Nucl Sci Tech. 2022;33:115. doi:10.1007/s41365-022-01097-9.

17. Hansson RC. Triggering and energetics of a single drop vapor explosion: the role of entrapped noncondens-able gases. Nucl Eng Technol. 2009;41(9):1215–22.

18. Song J, Wang C, Chen B, Li M, Shen Z, Wang C. Phenomena and mechanism of molten copper column interaction with water. Acta Mech. 2020;231:2369–80. doi:10.1007/s00707-020-02667-x.

19. Zyszkowski W. Experimental investigation of fuel-coolant interaction. Nucl Technol. 1977;33:40–59. doi:10.13182/NT77-A31762.

20. Nelson LS, Duda PM. Steam explosions experiments with single drops of iron oxide melted with CO_2–laser. High Temp–High Press. 1982;14:259–22.

21. Dombrovsky LA. Steam explosion in nuclear reactors: droplets of molten steel vs core melt droplets. Int J Heat Mass Transf. 2017;107:432–8. doi:10.1016/j.ijheatmasstransfer.2016.11.064.

22. Pitblado RM, Woodward JL. Highlights of LNG risk technology. J Loss Prev Process Ind. 2011;24(6):827–36. doi:10.1016/j.jlp.2011.06.009.

23. Vavilov SN, Vasil'ev NV, Zeigarnik Yu A, Lidzhiev EA. Experimental studies of phenomena occurring during vapor explosion triggering. Therm Eng. 2024;71(7):600–8. doi:10.1134/S0040601524700113.

24. Klimenko AV, Vavilov SN, Vasil'ev NV, Zeigarnik Yu A, Skibin DA. Vapor explosions: experimental observations of the spontaneous triggering phase. Doklady Phys. 2022;67(3):67–9. doi:10.1134/S1028335822010025.

25. Vavilov SN, Vasil'ev NV, Zeigarnik Yu A, Klimenko AV, Skibin DA. Spontaneous triggering of vapor explosion results of experimental studies. Therm Eng. 2022;69(7):484–9. doi:10.1134/S0040601522070072.

26. Vavilov SN, Vasil'ev NV, Zeigarnik Yu A. Vapor explosion: experimental observations. Therm Eng. 2022;69(1):66–71. doi:10.1134/S0040601522070072.

27. Uršič M, Leskovar M. Investigation of challenges related to vapour explosion modelling in sodium. Nucl Eng Des. 2020;363:110646. doi:10.1016/j.nucengdes.2020.110646.

28. Ciccarelli G, Frost DI. Fragmentation mechanisms based on single drop steam explosion experiments using flash X-ray radiography. Nucl Eng Des. 1994;146:109–32. doi:10.1016/0029-5493(94)90324-7.

29. Hansson RC, Park HS, Dinh TN. Dynamics and preconditioning in a single-droplet vapor explosion. Nucl Technol. 2009;167(1):223–34. doi:10.13182/NT09-A8864.

30. Kim B, Corradini M. Modeling of small-scale single droplet fuel coolant interactions. Nucl Sci Eng. 1988;98(2):16–28. doi:10.13182/NSE88-A23522.

31. Kazimi MS, Autruffe MI. On the mechanism for hydrodynamic fragmentation. Trans Am Nucl Soc. 1978;30:366–7.

32. Dombrovsky LA. Approximate model for break-up of solidifying melt particles due to thermal stresses in surface crust layer. Int J Heat Mass Transf. 2009;52(1–2):582–7. doi:10.1016/j.ijheatmasstransfer.2008.07.025.

33. Glazkov VV, Zhilin VG, Zeigarnik YA, Ivochkin YP, Igumnov VS, Sinkevich OA, et al. A study into development of instability and collapse of vapor layer on a heated solid hemispherical surface. High Temp. 2000;38:900–8. doi:10.1023/A:1004193307529.

34. Skripov V. Metastable liquids. New York and Toronto: J. Wiley; 1974.

35. Sinkevich OA. Waves on the surface of a vapor film under conditions of intensive heat fluxes. Phys Rev E. 2008;78:036318. doi:10.1103/PhysRevE.78.036318.

36. Schneider P. Engineering problems of thermal conductivity. Moscow: Publishing House of Foreign Literature; 1960. p. 1–478 (In Russian).

37. Krainov AY, Minkov LL. Computational methods for solving heat and mass transfer problems. Tomsk: Izdatelstvo STT; 2016. p. 1–92 (In Russian).

38. Gukhman AA. Application of similarity theory to the study of heat and mass transfer processes. Moscow: Higher School; 1974. p. 1–328 (In Russian).

39. Sher I, Harari R, Reshef R, Sher E. Film boiling collapse in solid spheres immersed in a sub-cooled S.R. liquid. Appl Therm Eng. 2012;36:219–26. doi:10.1016/j.applthermaleng.2011.11.018.

40. Yagov VV, Minko KB, Zabirov AR. Two distinctly different modes of cooling high-temperature bodies in subcooled liquids. Int J Heat Mass Transf. 2021;120838. doi:10.1016/j.ijheatmasstransfer.2020.120838.

41. Kanin PK, Yagov VV, Zabirov, Molotova IA, Vinogradov MM, Ryazantsev VA. On the vapor film destabilization mechanism during unsteady film boiling. High Temp. 2023;61:220–28. doi:10.1134/S0018151X23020086.

42. Ivochkin YP, Zeigarnik YA, Kubrikov KG. Mechanisms governing fine fragmentation of hot melt immersed in cold water. Therm Eng. 2018;65(7):462–72. doi:10.1134/S0040601518070029.